ISSN 2347 - 3983
Volume 11. No.4, April 2023
International Journal of Emerging Trends in Engineering Research
Available Online at http://www.warse.org/IJETER/static/pdf/file/ijeter021142023.pdf
https://doi.org/10.30534/ijeter/2023/021142023

Nanoproperties of Fly Ash based Geopolymer Concrete with Polypropylene Fibres

S. Subbiah Ilamvazhuthi [a*], R. Karthiga [b]
[a] Civil Engineering Department, Theni Kammavar college of Technology, Theni, 625531, Tamilnadu, India.
subbiahilamvazhuthi@gmail.com
[b] P. G and Research Department of Chemistry, CPA college, Bodinayakanur, Theni-625513, Tamilnadu, India.
skarthika1121@gmail.com

Received Date: February 23, 2023 Accepted Date: March 26, 2023 Published Date : April 07, 2023

ABSTRACT

Due of its amorphous-like properties, geopolymer concrete (GPC) possesses good quasi-brittle behavior. New studies has revealed that polypropylene fibre can also be used to concrete to increase the material's strength. In the ongoing work, a novel geopolymer concrete (FGPC) that was modified with polypropylene fibres been created as a replacement to conventional cement concrete. FT-IR, XRD, SEM, and the BET adsorption-desorption isotherm model were employed to evaluate the nanoproperties of the geopolymer concrete modified with polypropylene fibre. The maximum compressive strength will be most probably present in the developed concrete. Comparing FGPC to GPC and OPC, the pore capacity of FGPC was decreased by 0.025705 cm3/g and the water absorption was decreased. The substance in FGPC's SEM picture is denser than that in OPC and GPC. The interfacial bond between the minerals and the utilization of polypropylene fibre enhance the durability of geopolymer concrete, which was additionally supported by FTIR technique. Micro - cracks on the surface of OPC and GPC reduce compressive strength while enhancing porosity and water absorption.

Key words: Alkali activated cement, fly ash, Polypropylene fibres, structural properties

1. INTRODUCTION

When a strong alkali condition is available, alumina silicate substances including cement, marl, slag, fly ash, heated kaolin, and geopolymer were effective [1-3]. Inorganic geopolymers are the Si-O-Al composite with ceramic properties. The main composition of geopolymer is unstructured as related to naturally produced zeolitic polymers. The following explanation may be used to explain how amorphous geopolymers form when polymerization happens in an alkaline conditions: By splitting oxygen atoms between tetrahedral units, water is progressively split out and aligned to polymeric precursors. However, geopolymers exhibit a quasi-brittle behavior similar to OPC due to their ceramic-like characteristics; however, they have limited compressive strength [4, 5]. Thus, it is expected that remodelling the geopolymer will improve the strength and durability.

To enhance the strength, durability, and decrease the capacity for absorption of water in concrete and geopolymer cement as well as various other industrial products, polypropylene fibres are crucial elements. A greater level of setting and solidification, greater long-term characteristics and durability [6–8], good capacity to shatter hazardous metals [9], and improved resistance to acids and the impacts of fire [10] are only a few of the properties that this material offers. Their primary advantages include low price and environmental impact manufacturing, maximum temperature resistance, non-flammability, excellent quality for human use, and resilience to freezing and thawing cycles.

The distinctive characteristics of polymer concrete materials involve high strength and excellent bonding [11, 12]. In addition, excellent bonding with other materials [13], resistance to corrosion or chemical attack [14], low permeability, and quick curing [15] have made it a very alluring material in industries. It is frequently used in structural engineering and building applications.

In this study, polypropylene fibres were employed to develop a new geopolymer binding material. Furthermore, geopolymer concrete containing polypropylene fibres is the main point of focus for material characterization. A few information concerning material features, such as shape, surface area, crystalline nature, pore volume, and surface-active material, with the potential for high durability and strength, may be found in literature.

2. EXPERIMENTAL DESIGN

2.1. Materials

Directly from the Tuticorin Thermal Power Station in Tamil Nadu, India, Type F fly ash was worn. Table 1 contains the oxides percentage of type F fly ash that was obtained from the Regional Testing Laboratory in Madurai. Table 2 lists the

physical characteristics of the polypropylene fibres, including I specific gravity (2.82), (ii) fineness modulus (1.375), (iii) specific surface area (310 m2/kg), and (iv) fly ash density (1.4 kg/m^3). The grading curves were directly applied to fibre geopolymer concrete, and the coarse and fine aggregates utilized were the same as those used in the production of concrete. Na_2SiO_3 (sodium silicate) and NaOH (sodium hydroxide) solutions are blended to produce an alkaline liquid that is employed. This blend is prepared a day before it is required.

Table 1: Oxides percentage of fly ash

S.No	Composition	Percentage
1	SiO_2, Al_2O_3, Fe_2O_3	85.94
2	SiO_2	60.21
3	MgO	1.99
4	SO_3	2.19
5	Na_2O	0.39
6	CaO	1.94

Table 2: Physical properties of Polypropylene fibres

Effective Diameter	10 micron -1.0mm
Length	6 – 48 mm
Specific gravity	More than 1.0
Dosage	0.6 – 2.0 kg/cumec
Water absorption	Less than 0.45 %
Melting point	Less than 160° C

2.2. Specimen Preparation

Similar as far as how Portland cement concrete was created, traditional processes were employed to prepare Geopolymer concrete. 24 hours earlier to casting, the alkaline solution was formulated. The fly ash and the aggregates were homogenized and dried for approximately 3 minutes. The alkaline was added with the water reducer. For an additional four minutes, the dry components and liquid portion of the concrete were mixed together. On a vibrating apparatus, 150x300 mm cylinders and 150x150x150 mm cube specimens were cast and vibrated for 10 seconds [16].

2.3. Material Characterization

The surface-active groups in the concrete were detected using the JASCO - FT-IR - 460 plus spectrophotometer. An X-ray diffractometer (XRD; XPERT PRO X-RAY) with Cu K radiation at 25 oC was employed to investigate the crystalline structure of the concrete, and the structural assignments were made using the JCPDS powder diffraction files. The surface morphology of the concrete was conformed using the secondary and backscattered electron modes of JSM 6701F-6701, and the elemental analysis was also discovered. The surface area of about 250 mg of concrete was measured using Kr at liquid nitrogen temperature using a Micromeritics ASAP 2020 device. The samples were degaussed at 350 ºC for 18 hours prior to the measurements. The physisorption isotherms' surface area values were computed through using Brunauer-Emmet-Teller (BET) analysis.

2.4. Testing Program

2.4.1. Compressive Strength Test

According to IS:516-1959, concrete with dimensions of 150 mm x 150 mm x 150 mm was manufactured using and without using polypropylene fibre. These cubes then regularly vibrated using a table vibrator. The concrete that had been removed from the mould was heated for 24-36 hours before being sent out into the open. Using a compression testing machine with a 2000 kN capacity, the compressive strength of freshly prepared concrete was examined. The following equation was used to obtain the typical concrete compression strength. Three specimens were analyzed, and the average compressive strength was determined.

$$Compressive\ Strength\left(\frac{N}{mm^2}\right) = \frac{Ultimate\ Compressive\ Load}{Area\ of\ cross\ section\ of\ Specimen} ------1$$

2.4.2. Rapid Chlorine Penetration Test

Polypropylene Fibre was cast in concrete to construct concrete disc specimens of 100mm in diameter and the thickness of 50 mm (Fig. 1). After 24 hours, the disc concrete specimens' moulds were removed, and they were left to cure for 90 days in distilled water free of chloride. After curing, the disc concrete's chloride permeability was studied. Before testing, all of the disc-shaped concrete specimens were dried to eradicate all moisture.

Figure 1: Concrete disc specimen for RCP TEST

The two-compartment cell assembly gathers the disk-shaped concrete specimen, which is then assessed for air and water permeability. Then, following the method established in ASTM C1202, a DC power source of about 60V is impressed between anode (0.3 normality NaOH solutions) and cathode (3% NaCl solution) through the FGPC concrete specimens for 6 hours at periods of 30 minutes (Table 3).

Table 3: Charge processed by RCPT in accordance with ASTM C1202

S.No	Charge passed coulombs	Chloride ion penetrability
1	>4000	High
2	2000-4000	Moderate
3	1000-2000	Low
4	100-1000	Very low
5	<100	Negligible

Using the present readings, equation 2 is used to get the chloride permeability in coulombs at the end of 6 hours.

$$Q = 900\left(I_0 + 2I_{30} + 2I_{60} + \ldots\ldots\ldots + 2I_{300} + 2I_{330} + 2I_{360}\right) - - - -(2)$$

where,
Q = Charge passed (Coulombs)
I_0 = Current (amperes) immediately after voltage
I_t = Current (amperes) at t minutes after voltage

3. RESULT AND DISCUSSION

3.1. XRD

The XRD diffraction patterns of the OPC, GPC, and FGPC specimens are depicted in Fig. 2. The quartz, a component of cement concrete, and the anhydrous phases of cement with high crystallinity are the main components the diffractogrammes indicate [17]. A hump between 25°–30° and 70° has been identified by GPC, which indicates that geopolymerization and the hydration reaction of standard Portland cement have proceeded therein. The quantized that the GPC was primarily composed of fly ash-derived quartz crystal phases and minute amounts of microcline. An apparent change from a broad hump about 20° to 30° into acute peaks when GPC is activated with polypropylene fibre suggests the creation of a new phase of alimosilicate was seen.

The intercalation between geopolymer and fly ash was verified by the emergence of a new sharp peak with a shortened basal spacing value, showing the specimen FGPC's high thermal stability. The average crystallite size of OPC, GPC, and FGPC was calculated using the Debye's Scherrer equation [17]:

$$D = \frac{K\lambda}{\beta Cos\ \theta} - - - -(3)$$

Where K is the form factor, and is the most intense 2 peak's whole width at half height maximum (0.89). The incident angle and wavelength of X-rays are represented by and, respectively [18, 19]. It was found that the average particle size for OPC, GPC, and FGPC was 12.53 nm, 18.53 nm, and 43.32 nm. This implies that the geopolymerization concrete in Fig. 2 and Table .3 has been improved because polypropylene fibres had a greater capacity to link the fly ash particles.

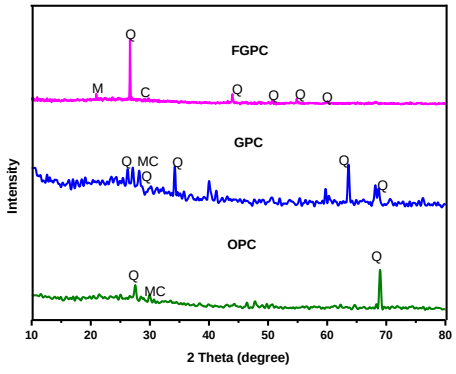

Figure 2: XRD pattern of OPC, GPC and FGPC

Table 4. Code and Name of the element in the OPC, GPC and FGPC

Code	Name	Reference No
Q	Quartz- SiO_2	00-046-1045
MC	Microcline-$KAlSi_2O_8$	00-019-0932
C	Calcite-$CaCO_3$	00-047-1743

3.2. FTIR

The FTIR spectra of the OPC, GPC, and FGPC are displayed in Figure 3. As shown, the bands of the OPC and GPC are comparable to the FGPC. The peak at 1000 cm^{-1} is related to the stretching vibration of Al-O and Si-O, which is caused by geopolymerization [22], and it becomes broad in FGPC as a result of the fly ash's dissociation from alkaline and polypropylene to make way for new specimens. The 3453 cm^{-1} and 1638 cm^{-1} peaks were built to extend H-OH and H-O-H. Alkaline NaOH aqueous stage spread on the geopolymeric surface is allowed to carbonate in the atmosphere at the pointed peak at 1460 cm^{-1}. At 558 cm^{-1} [23], the double-ring linkage's hump was evident. Si-O-Si bending, Si-O-Si and Si-O-Al asymmetric stretching vibration are each linked to the broad band at 445 cm^{-1} and 990 cm^{-1}, respectively. Al-O and Si-O correlations are assigned to the weak band at 670 cm^{-1} [24]. Polypropylene fibres were added, and it was noted that this improved polymerization resulted in the composites having good strength [23].

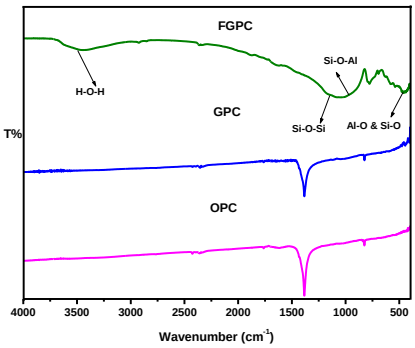

Figure 3 : FTIR spectrum of OPC, GPC and FGPC

3.3. SEM

An understanding of the morphology of geopolymers was gained from scanning electron microscopic investigations. Fig. 4 (a-c), which depicts the overall view of OPC, GPC, and FGPC, shows an amorphous geopolymer matrix that is mostly made up of Si, Al, Na, and Ca. For GPC and FGCP, the geopolymeric gel, which is proof of a geopolymerization reaction [24], was shown to form. The FGPC materials appear to be free of cavities and are comparatively dense when compared with the OPC and GCP materials displayed in Fig. 4(a-c). The basic mass of fly ash-based geopolymers has an amorphous phase and the presence of needle minor configurations. For fly ash-based geopolymers, however, Fig. 4 (b) shows that the aggregated nonuniform particles are quiet and that specific impacts of the surface interaction between the particles, which influences the aggregation, are carried about by the existence of polymer molecules in the interlamellar space. However, the proportions of amorphous phases that were likely formed concurrently during the preparation may have a significant impact on the morphology. This is because the addition of fly ash and geopolymer with NaOH increased compressive strength. The specimen's NaOH strengthens the silica and alumina leaching and causes the production of NASH gel, which increases the specimen's toughness. This leads to the conclusion that the fly ash source only influences

the reaction between the activating solution and fly ash, which may weaken OPC's compressive strength. Although the surface is smooth and the matrix is heavily geopolymerized, the addition of fly ash-based geopolymer enhances the compressive strength of the FGPC.

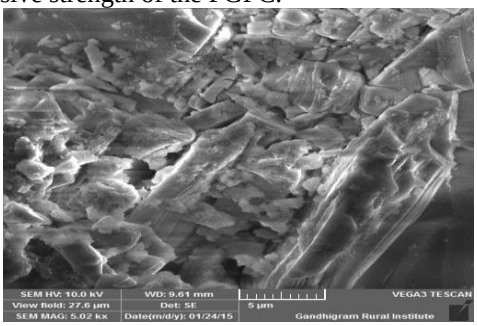

Figure 4 (a): SEM image of OPC

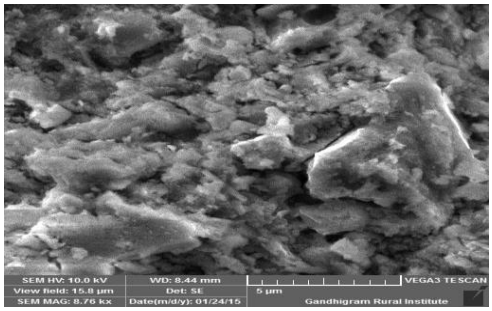

Figure 4 (b): SEM image of GPC

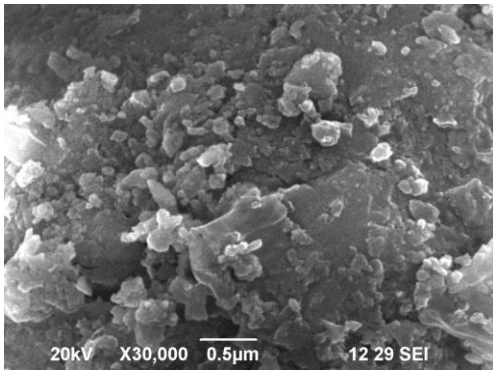

Figure 4 (c): SEM image of FGPC

3.4. Surface Properties

Fig. 5 summarises the specific surface area (BET method) results for OPC, GPC, and FGPC (a-c). Concrete voids may be filled with either air or water. Concrete pores are readily seen as voids. The adsorption of water on both the external and internal surfaces of the concrete, which gives an indication of the whole adsorption capacities of specimens, causes the pores to open up, generally speaking, making the concrete weaker. BET measurement provides data on the size of exterior surfaces. Using the B.E.T. equation, the surface area (SB.E.T. (m^2/g)) is determined to be 31.3379 m^2/g, 17.7582 m^2/g, and 4.7421 m^2/g for the OPC, GPC, and FGPC, respectively, which follow type IV with H2 hysteresis loop [25]. With the addition of fly ash and geopolymer, it is shown that the material's obvious cracks are minimized, and the surface area decreases as a result of less water absorption, increasing the compressive strength. It is clear from the SEM examination that the geopolymer is the one that is the most mesoporous, and the addition of fly ash reduces the surface area (Fig. 5). The result reveals that the BET surface area of the FGPC is smaller than that of the OPC and GPC. The mesoporous feature of the material also made it possible for reactants to diffuse quickly and water molecules to absorb less, increasing the concrete's strength. These clear findings show that the geopolymers have generally similar properties in the nanometric range and are not very dependent on the conditions of preparation. Only the geopolymer patterns are unique. Due to the coexistence of geopolymers and the N-A-S-H phase, the pore size in these materials decreases there. In terms of the total volume, the observed pore size ranges from 43 to roughly 60% and a comparision of Specific surface area, Pore volume and Crystalline size was shown in Table. 5

Table 5: Surface area, pore diameter, crystalline size

Samples	Specific surface area (m^2/g)	Pore Volume (cm^3/g)	Crystalline size (nm)
OPC	31.3379	0.153986	12.53
GPC	17.7582	0.116890	18.53
FGPC	4.7421	0.025705	43.32

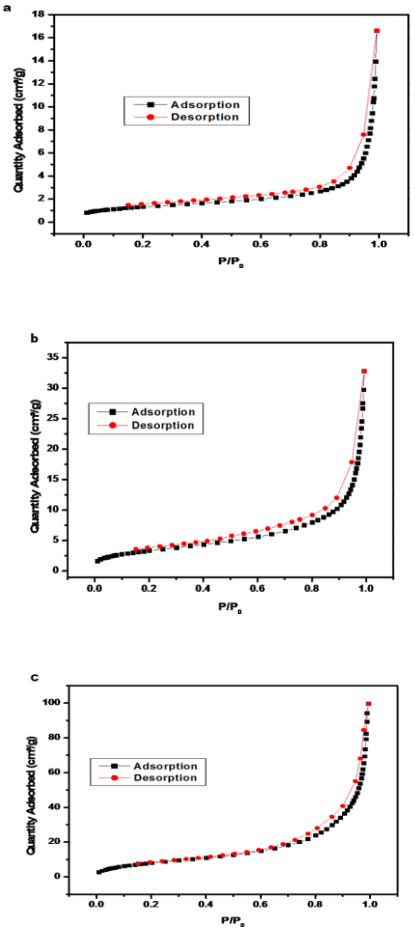

Figure 5: Nitrogen adsorption–desorption isotherms (a) OPC(b) GPC (c) FGPC

3.2. TEST RESULT

3.2.1. Compressive Strength

Experimental research on the strength developed during the course of 3, 7, 14, 28, 56, 90, and 180 days on OPC, GPC, and FGPC concrete cubes is conducted for each age, and the mean results are provided numerically and schematically in Table 6 and Fig. 6. The test findings demonstrate an increase in FGPC compressive strength for mixtures made with polypropylene fibre. The findings indicate that as age rises, the range in strength gain declines and nearly returns to normal after 56 days. The improved binding strength between the surfaces of the fibre and concrete cubes is what gives FGPC its increased compressive strength. As a result, the matrix and the polypropylene fibres' hard-impressed surface may have a stronger bond [26].

Table 6: Behaviors of FRGP concrete under compression

S.No	Mix IDs	Compressive strength in MPa						
		3 Days	7 Days	14 Days	28 Days	56 Days	90 Days	180 Days
1	OPC	6.00	21.00	27.00	29.00	30.20	30.40	30.62
2	GPC	10.00	26.00	32.00	33.55	34.32	34.85	34.98
4	FGPC	13.00	33.00	36.00	39.26	40.45	41.25	41.36

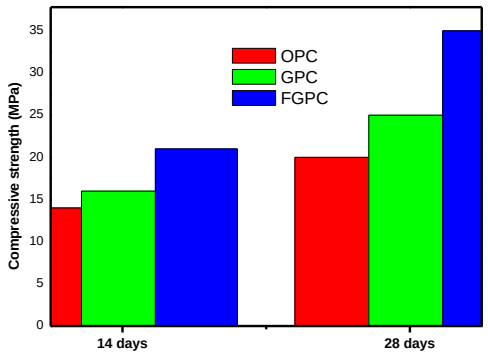

Figure 6: Compressive strength comparison between OPC, GPC and FGPC

3.2.2. Rapid Chloride Penetration Test

For a variety of specimens, concrete disc specimens of 100 mm in diameter and 50 mm in thickness were cast. For various Mix IDs, the chloride diffusion rate was reviewed in Table 7 in terms of charge transmitted in Coulombs. 28 days, 56 days, and 90 days were used for the test. For OPC, the highest average charge passed over 28 days was 423.25 coulombs, and the lowest average charge passed over 90 days was 408.76 coulombs. For FGPC, the highest charge that was passed was 371.45 coulombs on day 28, and the lowest charge that was passed was 329.86 coulombs on day 90. Thus, the inclusion of polypropylene fibre improves GPC behaviour by preventing chloride penetration and increasing endurance. This may also have an impact on the design of a secondary C-S-H gel and the composition of an improved transition zone, which lowers the coefficient of chloride migration in concrete. At a later adults, polypropylene fibres performed much better in the improvement of chloride diffusivity. This is in line with previous researchers' investigation, which found that the substitution of polypropylene fibres only reduced the porosity of concrete at a later stage of curing.

Table 7: RCPT test on FRGP concrete

Mix IDS	Average charge passed in Coulombs			RCPT Rating As per ASTM C1202
	28 days	56 days	90 days	
OPC	423.25	415.54	408.76	Very low
GPC	413.75	403.66	399.75	Very low
FGPC	371.45	340.87	329.86	Very low

4. CONCLUSION

In recent years, polypropylene fibre has been used in concrete constructions due to its improved performances and favourable cost-benefit ratio. The benefit also applied to fibre geopolymer concrete. BET methods are used to measure porosity. The holes were discovered to be evenly distributed across the samples for both additives. The differences in pore size for samples with and without the addition of polypropylene fibre have been demonstrated by the findings of BET and SEM. In comparison to OPC and GPC, the pore volume and surface area of the FGPC sample are low. The use of Fiber Geopolymer Concrete has been shown to have various financial advantages in the research. Increased impact resistance and tensile strength give the ability to lower the weight and thickness of structural components, which should also minimize damage from handling and transportation. The study's behavior will be discussed in the future and it can be further expanded to include slabs, beams, and columns. The results indicate that the decreased capillary porosity and lower inner conductivity of pores caused by the inclusion of PP fibres result in a reduction in the chloride diffusivity of concrete.

REFERENCES

[1] J.E. Bolander, S. Berton, **Simulation of shrinkage induced cracking in cement composite overlays,** Cem. Conc. Res. Vol. 26, pp. 861–871, 2004.

[2] J.A. Barros, V.M. Cunha, A.F. Ribeiro, J.A. Antunes, **Post-cracking behaviour of steel fibre reinforced concrete.** Mater Struct 2005; 38:47–56.

[3] D. Hardjito, S.E. Wallah, D.M. Sumajouw, B.V. Rangan, **On the development of fly ash-based geopolymer concrete,** ACI Mater. J. Vol. 101 (6), pp. 467-472, 2004.

[4] J. DAvidovits, **Soft mineralogy and Geopolymer, proceedings of the Geopolymer 88 international conference,** The university de Technologie, Compiegne, France, 1988.

[5] D.P. Dias, C. Thaumaturgo, **Fracture toughness of geopolymeric concretes reinforced with basalt fibers**, Cem. Concr. Compos. Vol. 27, pp. 49–54, 2005.

[6] F. Puertas, T. Amat, A. Fernández-Jiménez, T. Vázquez, **Mechanical and durable behaviour of alkaline cement mortars reinforced with polypropylene fibres**, Cem. Concr. Res. Vol. 33, pp. 2031–2036, 2003.

[7] Z. Zhang, X. Yao, H. Zhu, S. Hua, Y. Chen, **Preparation and mechanical properties of polypropylene fiber reinforced calcined kaolin-fly ash based geopolymer,** J. Cent. S. Univ. Technol. Vol. 16, pp. 49–52, 2009.

[8] T. Bakharev, **Durability of geopolymer materials in sodium and magnesium sulfate solutions,** Cem. Concr. Res, Vol. 35, pp. 1233–1246, 2005.

[9] E. Alvarez Ayuso, X. Querol, F. Plana, A. Alastuey, N. Moreno, M. Izquierdo, O. Font, T. Moreno, S. Diez, E. Vázquez, M. Barra, **Environmental, physical and structural characterisation of geopolymer matrixes synthesised from coal (co) combustion fly ashes,** J Hazard Mater, Vol. 154, pp. 175-183, 2008.

[10] T. W. Cheng, J.P. Chiu, **Fire resistant geopolymer produced by granulated blast furnace slag,** Miner Eng, Vol. 16 pp. 205–210, 2003.

[11] J.M.L. Reis, **Mechanical characterization of fiber reinforced polymer concrete**, Mater Res, Vol. 8 (3), pp. 357–360, 2005.

[12] M.M. Shokrieh, M. Heidari-Rarani, M. Shakouri, E. Kashizadeh, **Effects of thermal cycles on mechanical properties of an optimized polymer concrete,** Constr. Build. Mater, Vol. 25 (8), pp. 3540–3459, 2011.

[13] M.C.S. Ribeiro, J.M.L. Reis, A.J.M. Ferreira, A.T. Marques, **Thermal expansion of epoxy and polyester polymer mortars—plain mortars and fibre-reinforced mortars,** Polym Test, Vol. 22 (8) pp. 849–857, 2003.

[14] M.C.S. Ribeiro, C.M.L. Tavares, A.J.M. Ferreira, **Chemical resistance of epoxy and polyester polymer concrete to acids and salts,** J Polym Eng, Vol. 22 (1), pp. 27–43, 2002.

[15] J.M.L. Reis, A.J.M. Ferreira, **The influence of notch depth on the fracture mechanics properties of polymer concrete,** Int J Fract Vol. 124, pp. 33-42, 2003.

[16] A. Camille, D. Pauls, **Experimental study of epoxy repairing of cracks in concrete,** Constr Build Mater 21 (2007) 157–63.

[17] D.W. Fowler, **Polymers in concrete: a vision for the 21st century,** Cem Concr Compos 21 (1999) 349–467.

[18] R. Karthiga, C. Mutharasu, A. Velmurugan, P. Sambathbabu, **Aerva Lanata Mediated Phyto-Fabrication of SnO_2 Nanoparticles and Evaluation of Their Antimicrobial Activity,** Inter. J. Res Analyt. Review, Vol 9(2) pp. 601-606, May,2022.

[19] R. Karthiga, A Sudha, **Green Synthesis of ZnO Nanoparticles Using *Sollanam Santhocarbom* to Study Its Solar photocatalytic Activity,** Inter. J. Sci. Resea. Vol.6 (6), pp. 2370-2376, June, 2017.

[20] A.J. Boyd, S. Mindess, J. Skalny, **Designing concrete for durability,** Mater. Constr.51 (2001) 263–264.

[21] K. Wang, D. Jansen, S. Shah, A. Karr**, Permeability study of cracked concrete,** Cem. Concr. Res. Vol.27 (3), pp. 381–393, 1997.

[22] N.J. Brooke, L.M. Keyte, W. South, L.M. Megget, J.M. Ingham, **Seismic performance of 'green concrete' interior beam-column joints,** Proceeding of Australian Structural Engineering Conference (ASEC) 2005, Newcastle.

[23] K. Uma, R. Anuradha, R. Venkatasubramani, **Experimental investigation and analytical modeling of reinforced geopolymer concrete beam,** Int. J. Civ. Struct. Eng. (2012) 3.

[24] M.D.J. Sumajouw, B.V. Rangan, **Low calcium fly ash-based geopolymer concrete: reinforced beams and columns,** Research report GC-3 2006, Faculty of Engineering, Curtin University of Technology, Perth, Australia.

[25] D. Zaharaki, K. Komnitsas, and V. Perdikatsis, **Use of analytical techniques for identification of inorganic polymer gel composition,** Journal of Material Science, vol. 45, pp. 2715-2724, 2010.

[26] S. Subbiah ilamvazhuthi, G.V.T. Gopalakrishna, **Performance of geopolymer concrete with polypropylene fibres,** International journal of innovations engineering and technology, vol. 3(2) pp. 148-156, 2013.